THESIS FOR THE DEGREE OF LICENTIATE OF ENGINEERING

in

Thermo and Fluid Dynamics

Reduction of heat transfer and heat load in internal combustion engines

JOOP SOMHORST

Division of Combustion and Propulsion Systems

Department of Mechanics and Maritime Sciences

CHALMERS UNIVERSITY OF TECHNOLOGY

Gothenburg, Sweden 2019

Reduction of heat transfer and heat load in internal combustion engines

JOOP SOMHORST

Thesis for the degree of Licentiate of Engineering 2019:01
ISSN 1652-8565

Division of Combustion and Propulsion Systems
Department of Mechanics and Maritime Sciences
Chalmers University of Technology
SE-412 96 Gothenburg
Sweden
Telephone +46 (0)31 772 1000

Chalmers Reproservice
Gothenburg, Sweden 2019

Reduction of heat transfer and heat load in internal combustion engines

JOOP SOMHORST

Division of Combustion and Propulsion Systems
Department of Mechanics and Maritime Sciences
CHALMERS UNIVERSITY OF TECHNOLOGY

Abstract

Thermal insulation of the combustion chamber in an engine has great potential to reduce fuel consumption and CO_2 emissions. Research on thermal barrier coatings (TBC) has been performed since the early eighties to address this potential. However, reported results for engine efficiency improvements show a large spread and there is no consensus on the actual benefits of the application of TBCs. Recent work indicates that a high surface roughness, typical for many TBCs, increases fuel consumption.

The purpose of the work described in this thesis was to make an accurate assessment of the indicated efficiency and to quantify the effect of surface roughness for two representative thermal barrier coatings applied on the piston crown in a single cylinder light duty diesel engine. Cylinder pressure data and measured heat losses to the piston cooling oil formed the basis for the evaluation.

A robust and automated measurement method was developed and combined with statistical modeling of the data. This approach increased the precision of the results and made it possible to separate the effect of different factors like surface roughness, compression ratio and coating application.

The compression ratio is an important variable in the analysis of the cylinder pressure data. However, it was not possible to measure the volume of the coated pistons accurately due to the porosity of the coatings. A method to determine the compression ratio from motored pressure traces was found in literature and further developed. This unique method does not require an estimation of the heat losses and is therefore especially suited for pistons with thermal insulation.

The indicated efficiency was measured with a 95% confidence interval of ±0.1 percentage point. Analysis of the results showed that the typically high surface roughness of plasma sprayed zirconia and anodized alumina increases fuel consumption by up to 1%. The high surface roughness enhanced heat losses and delayed combustion. The coatings themselves reduced heat losses to the combustion chamber walls and increased exhaust enthalpy, but they did not improve indicated efficiency.

Keywords: engine, efficiency, emissions, heat transfer, thermal barrier coating, TBC, surface roughness, zirconia, alumina

List of publications

This thesis is based on the work contained in the following publications:

Paper I Somhorst, J., Oevermann, M., Bovo, M., and Denbratt, I., "A Method to Evaluate the Compression Ratio in IC Engines with Porous Thermal Barrier Coatings," *SAE Technical Paper 2018-01-1778*, 2018, doi:10.4271/2018-01-1778

Paper II Somhorst, J., Oevermann, M., Bovo, M., and Denbratt, I., "Evaluation of thermal barrier coatings and surface roughness in a single cylinder light duty diesel engine", *International Journal of Engine Research*, 2019. (submitted for review).

Acknowledgements

I would like to start with the acknowledgement of the Volvo Industrial PhD Program, started in 1999, facilitating the education of about 30 to 40 PhD students each year. It is great to get the chance to work in both worlds, industry and academia.

From Volvo I would also like to give special thanks to some of my colleagues: Lucien Koopmans who gave me the opportunity to embark on the same voyage he made 14 years ago. Carolin Wang-Hansen, my manager, really helped me to keep up the motivation and made sure I could focus on my PhD project within the dynamic world at Volvo Cars. Mirko Bovo, thank you for your supervision, your positive humor and the spot on metaphors. I will never forget the one with the Ferrari and the clutch.

I could not have done the engine experiments at Volvo Cars without the help of Janne and Christer, the legendary single cylinder engine mechanics. We were changing pistons and running tests every day, for three weeks in a row. The test cell was not unlike a formula one pit stop. Tools driven by compressed air, making loud whizzing noises when the engine was disassembled and reassembled in an amazing speed.

From Chalmers, I would like to start with thanking Ingemar Denbratt for making it possible to do my PhD within the CERC program and his positive attitude towards my project. Michael Oevermann, my main supervisor, you have given me good advise and valuable feedback on my work, even though we come from very different backgrounds and fields of experience.

I also need to thank Jon-Anders, with whom I share the 'Volvo room' at Chalmers. I really appreciated all of the shared lunches and the interesting discussions about anything, including combustion engines.

Finally, I am truly grateful to my wife Ann-Charlotte and my daughter Louise for the support and the understanding of my physical and mental absence during the intense periods of measuring and writing. You are the best!

Table of contents

1 Introduction

1.1 Motivation

Volvo Car Corporation has been producing its own diesel engines since 2000, starting with the 5-cylinder 'new engine diesel' (NED5). At that time, with a common rail fuel injection system capable of delivering 1600 bar injection pressure and a specific performance of 50 kW/L, it was a very modern and powerful engine. Since then, the performance of the company's engines has steadily increased, and with downsizing to reduce fuel consumption, the specific power has increased even faster. The specific performance of the current 4-cylinder VED4 is 86 kW/L, an increase of over 70% in 15 years. The power density has reached a point where the heat load from the combustion on the cylinder head and piston is becoming critical. It is difficult to increase cooling performance further, and advanced (expensive) materials are required.

As awareness of global warming problems has increased, increasingly strict legislation has been introduced regarding both use of renewable fuels and CO_2 emission limits. The fleet average limits for CO_2 emissions from passenger cars (produced by each manufacturer supplying the EU market) in the NEDC (New European Driving Cycle) are 130 g/km by the end of 2015, 95 g/km by 2021, and an expected target for 2025 is 75 g/km. Similar legislation has been passed in Japan, China, the USA, Canada, India, Mexico, Brazil and South Korea, with more countries to follow.

One way to reduce (local) CO_2 emissions and meet the legislation requirements is to introduce electrification of the powertrain, but this is still very costly. Hence, there will be a limited range of affordable hybrid and fully electrical vehicles in the near future and combustion engines will be needed for at least a few more decades. Thus, the car industry is still making intense efforts to reduce the fuel consumption of both gasoline and diesel engines in order to meet the future CO_2 emission reduction targets at affordable costs.

One of the energy conversion losses in the internal combustion engine is heat transfer from the hot cylinder charge and exhaust gas to the surrounding walls. Figure 1. shows the typical heat flow distribution in a combustion engine. If this heat loss to the coolant can be reduced, more heat can be converted to work and the heat load on the exposed engine components would be reduced. Both fuel economy and engine durability would improve and it would be possible to increase specific power. Moreover, the increased temperature of the exhaust gases can give more energy to the exhaust turbine and enable faster catalyst light of for improved emission conversion. Additionally, when less heat is transferred to the coolant, the cooling system dimensions and weight can be reduced.

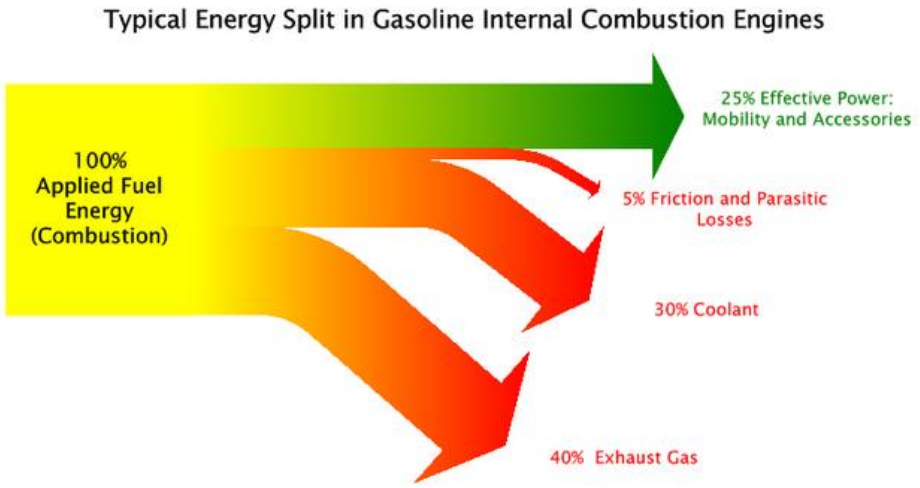

Figure 1. Engine energy flow distribution; typical coolant losses are between 20 to 35% of the total fuel energy.

1.2 Objectives

The main objectives at the start of this PhD project were two-fold:

1. Reduction of fuel consumption and CO_2 emissions with 2% by increasing the indicated efficiency.
2. Improved engine durability at high power output, with respect to components with high thermal loading. This might be achieved with very local measures in the combustion chamber.

The means to be researched and developed were thermal barrier coatings and surface structures that reduce the heat flow from hot gas to the walls.

2 Background

2.1 Principles of heat transfer

There are three ways to transfer heat - thermal energy - between different objects: conduction, convection and radiation. Figure 2 illustrates this with an example for a solid wall between two fluids where the temperature in the fluid on the left is higher than the temperature in the fluid on the right. The incident radiation can come from the fluid, but more often it will come from a radiant source at high temperature, not shown in this picture. Each mode of heat transfer is explained in more detail in the following subsections.

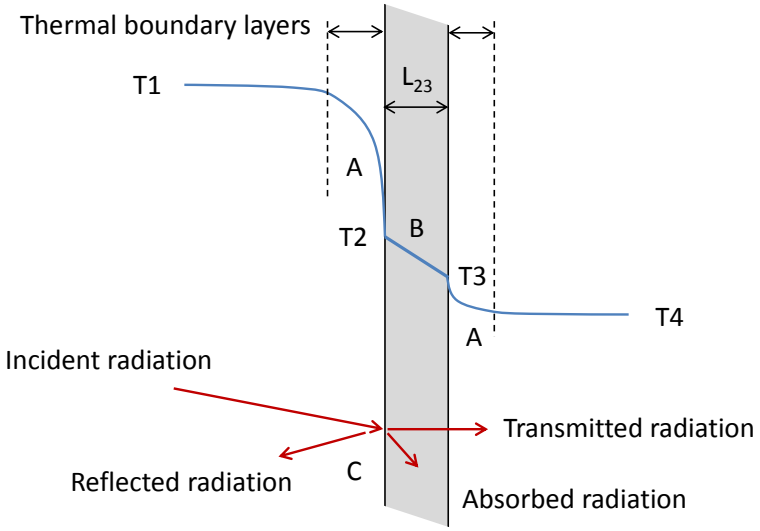

Figure 2. An example of heat transfer between two fluids separated by a solid wall showing A: convection, B: conduction and C: radiation.

2.1.1 Conduction

Heat conduction takes place where the transport of thermal energy is done by direct exchange of kinetic energy between molecules. Although this type of heat transfer also takes place in fluids it is most commonly used to describe heat transfer in solids, where it is the only way to transport heat, apart from radiation in transparent solids. In one-dimensional form, for a distance L_{23}, a thermal conductivity k and a surface area A, the equation for the rate of heat transfer (steady state) from location 2 to 3 is:

$$\dot{Q}_{cond} = \frac{k}{L_{23}} A(T_2 - T_3) \quad (1)$$

For the transient heat transfer in solids, two more properties are of significance: thermal diffusivity a and thermal effusivity e. Thermal diffusivity is a measure for the time it takes for heat to travel through a material, or the time it takes to reach thermal

equilibrium. The expression below shows that a material with high thermal diffusivity has a high ratio between conductivity and volumetric heat capacity.

$$a = \frac{k}{\rho\, c_p} \tag{2}$$

The thermal effusivity e defines the capability of a material surface to exchange heat, for example between to solid bodies in contact. When both thermal conductivity and volumetric heat capacity are high, heat can be exchanged fast, while the surface temperature remains relatively unchanged. A material at room temperature with high effusivity feels cold, like for example aluminum, as it removes heat quickly from the skin while maintaining a low surface temperature. Low effusivity is important for low dynamic heat exchange. An example is the use of wood as material for floors and furniture.

$$e = \sqrt{k\, \rho\, c_p} \tag{3}$$

Table 1 gives the thermal properties related to thermal conduction for some well known materials. There is a big variation in conductivity, the differences in volumetric heat capacity for the solids are small in comparison.

From the table it can be seen that aluminum is a very suitable material for cooling finns on electronic components, glass is an excellent material for hot drinks and wood can be used as a 'warm' material in our house interiors. And still air of course is a perfect insulator in for example clothing.

Table 1. Thermal properties for pure aluminum, iron, glass, wood and air at 1 atm. and 25 °C. Source: [1]

	k	$\rho \times c_p$	$a \times 10^5$	e
	[W/m.K]	[kJ/m^3.K]	[m^2/s]	[W.s$^{0.5}$/m^2.K]
Al (pure)	237	2440	9.71	24047
Fe (pure)	80	3518	2.27	16776
Glass	1.4	1875	0.08	1620
Wood (average)	0.13	1125	0.01	382
Air	0.026	1.2	2.14	5.6

2.1.2 Convection

In fluids, heat is transported by conduction, diffusion and advection, grouped together under the term convection. Convection transfers heat from one region to another, or to a solid surface in Figure 2 shown in the regions labeled A. In the introduction here, only forced convection in turbulent flows will be discussed, as this is the case for the internal flows in a combustion engine.

In most flow cases a boundary layer develops between the bulk flow and the wall. The fluid velocity at the wall is equal to zero and heat transport perpendicular to the surface will be reduced as the fluid moves more and more parallel closer to the surface. In case of a turbulent flow, three regions can be defined in the boundary layer. The near-wall viscous laminar sublayer, the transitional buffer layer and the turbulent layer, with increasingly larger flow structures away from the wall.

In the boundary layer heat is transferred by advection and conduction. Heat transfer by diffusion can mostly be neglected. Equation (4) shows the general relation for the convective heat transfer. As for conduction, heat transfer increases linear with surface area and temperature difference.

$$\dot{Q}_{conv} = h_c\, A(T_1 - T_2) \tag{4}$$

The heat transfer coefficient h_c for forced, turbulent convective flow is a function of a number of parameters shown in Equation (5), representing bulk flow velocity U, a typical length scale L, thermal conductivity k, dynamic viscosity μ, specific heat capacity c_p, density ρ and surface roughness ϵ.

$$h_c = f\big(U, L, k, \mu, c_p, \rho, \epsilon, \dots\big) \tag{5}$$

The rather complex expression for the heat transfer can be simplified by using dimensionless numbers, a common approach in the field of fluid dynamics. The Nusselt number is defined in Equation (6), and can be expressed in the Reynolds number and Prandtl number, Equations (7) to (9).

$$Nu = \frac{\text{total convective heat transfer}}{\text{conductive heat transfer}} = \frac{h_c L}{\mu} \tag{6}$$

$$Nu = f(Re, Pr, \dots) \tag{7}$$

$$Re = \frac{\text{inertial forces}}{\text{viscous forces}} = \frac{\rho\, U\, L}{\mu} \tag{8}$$

$$Pr = \frac{\text{momentum diffusion rate}}{\text{heat diffusion rate}} = \frac{c_p\, \mu}{k} \tag{9}$$

In combustion engines, the in cylinder charge flow is highly turbulent. Often a comparison is made with turbulent pipe flow where correlations have been derived to calculate the convective heat transfer coefficient.

$$Nu = 0.023\, Re^{0.8} Pr^{0.33} \tag{10}$$

The Reynolds number is a measure of turbulence level of the flow and depends on bulk flow velocity, a characteristic length and kinematic viscosity μ/ρ. The Prandtl number is defined by fluid properties only. For most gases, Pr is fairly constant for a large range of pressures and temperatures. Equation (10) is often used as the basis for engine heat transfer correlations.

Surface roughness plays an important role in convective heat transfer. It can increase heat transfer significantly by increasing the effective contact surface area between fluid and solid and by increasing turbulence in the boundary layer. To have an effect on the turbulence, the surface roughness should protrude through the laminar, viscous sublayer into the transitional buffer region where the turbulence starts to increase. If the aim is to increase heat transfer, the typical surface roughness height should be at least 2-3 times the thickness of the laminar sublayer [1].

The aim with this research however, is the opposite: the target is to minimize heat transfer. For a wall to be considered smooth, the surface roughness profile should be contained within the viscous laminar sublayer. The laminar sublayer thickness itself depends on flow conditions and fluid properties. The main factor is the turbulence level; reduction of the Reynolds number will increase laminar boundary layer thickness. As a consequence, low surface roughness is important in flow cases with high Reynolds numbers if low heat transfer is desired.

Often the roughness height is divided by the typical length scale of the flow to get the dimensionless roughness parameter: ϵ/L.

2.1.3 Radiation

Heat transfer by radiation does not require direct contact between the objects and occurs instantly. Every object with a temperature higher then 0 Kelvin emits radiation, the quantity increasing exponentially with temperature. Equation (11) shows the Boltzman relation for the net heat transport between two infinite parallel plates with temperature T_1 and T_2. The variable σ is the Boltzman constant. In this simple form the plates are assumed to behave as black bodies. The expression shows that radiation becomes exponentially more significant at high temperatures.

$$\dot{Q}_{rad} = \sigma\, A(T_1^4 - T_2^4) \tag{11}$$

Real objects do not emit as much radiation as a black body and do reflect and transmit radiation as well. To account for real world properties there are a number of efficiency factors related to radiation namely: emissivity ε, absorbtivity α, reflectivity ρ and transmissivity t. The effect of finite surfaces exchanging radiation energy is described by a form factor ξ.

The calculation of heat transfer by radiation is rather complex and often neglected in engine modeling, although it can be of importance for engine operating conditions with high load and high soot levels in the cylinder.

2.2 Heat transfer in combustion engines

2.2.1 Heat transfer correlation models

Based on the correlation for turbulent pipe flow (10), Hohenberg and Woschni among others have developed empirical correlations for engine heat transfer. These models were tuned with a large range of engines and have proven very useful for engine design. The correlation for the heat transfer coefficient in equation (12) by Woschni [2] shows the dependency on the cylinder bore B, charge pressure p and charge temperature T. The variable w represents the turbulence level and is a function of mean piston speed and accounts for combustion generated turbulence.

$$h_c = 3.26 \frac{p^{0.8} w^{0.8}}{B^{0.2} T^{0.55}} \tag{12}$$

From the general heat transfer theory and with this validated experimental correlation for the heat transfer coefficient, the general measures for heat transfer reduction can be listed:

- reduction of wall surface area
- decrease of charge temperature
- increase of wall temperature
- reduction of charge turbulence
- low surface roughness
- high reflectivity of the wall surface

In relation to insulation with thermal barrier coatings, the wall surface temperature will increase with low thermal conductivity and low volumetric heat capacity.

2.2.2 Impinging jet

Heat transfer in direct injected diesel engines is highly inhomogeneous. This aspect is not captured by the zero-dimensional correlations like the expression from Woschni. Heat transfer is particularly high in the region of spray impingement on the combustion chamber wall. Spray velocity and temperature are very high and the boundary layer at this location is typically very thin. This aspect is important when considering where to apply thermal insulation.

2.2.3 Adiabatic engines

The pioneering work within the field of combustion chamber insulation was performed in the early 80's by Kamo and Bryzik [3–6]. The subject of their work was actually not to increase indicated efficiency. Their goal was to create an adiabatic engine that would not include a cooling system and that had a turbocompound system to make use of the redirected exhaust heat. Insulation was achieved by the use of ceramic monoliths or steel with low thermal conductivity like Inconel, in combination with air gap insulation.

There were similar research projects with adiabatic engines at that time having focus on increasing indicated efficiency. Both big improvements and deteriorations of indicated efficiency were reported. In general there was a large spread in published research results [ref].

One of the major issues with this concept was the permanently elevated temperature of the combustion chamber walls. This resulted in poor volumetric efficiency, deteriorated combustion and increased NO_x emissions. Other problems were durability of the ceramic engine parts and lubrication of the piston-liner contact [ref].

2.2.4 Thermal barrier coatings

The alternative to the adiabatic engine was to develop relatively thin thermal barrier coatings. Morel et al. [7] studied the cyclic wall temperature behavior and formulated expressions for the penetration depth of the temperature variations and the so called temperature swing of the surface, shown in Equations (13) and (14). A thermal barrier coating that is capable of following the charge temperature does not have to be thicker than the penetration depth. A TBC thickness higher than the penetration depth would only increase the average surface temperature. As a reference: a typical penetration depth for aluminum is in the range of 1 mm.

$$\text{penetration depth:} \quad \delta_p \propto \sqrt{a\ t} \qquad or \qquad \delta_p \propto \sqrt{\frac{k}{\rho\ c_p}\ t} \tag{13}$$

$$\text{temperature swing:} \quad \Delta T \propto \frac{1}{\sqrt{\rho\ c_p\ k}} \tag{14}$$

This temperature concept required materials with low thermal conductivity and low heat capacity. Most of the materials were ceramics, metal oxides, applied by plasma spraying, thermosetting slurry coatings or hard anodizing of aluminum. Many engine experiments have been performed with different types of coatings with varying success.

Thermal insulation of the combustion chamber with TBCs has been investigated by many researchers, with experiments as well as thermodynamic process simulations. Most of the experiments show an increase in exhaust temperature and a reduction in heat losses to the coolant, as expected and predicted by simulations. However, the experimental results for the engine efficiency show a large variation and there is no general agreement on the benefit of TBCs for indicated efficiency [8–10]. Moreover, it seems that, on average, the effect of insulation with TBCs on indicated efficiency is limited.

The variation in the reported benefits from TBCs is partly related to the large range of tested engine hardware, the variation in engine operating conditions and the engine technology level used in the experiments. Another cause for the varying results from experiments is the increased wall temperature that follows with insulation. This temperature increase results in a higher charge temperature and lower charge density. For compression ignition (CI) engines this can lead to a lower air-fuel ratio and differences in ignition delay, fuel-air mixing, emission formation and oxidation. Especially combustion phasing and the rate of heat release have a significant effect on the indicated efficiency. How these secondary effects change the efficiency is engine specific and depending on engine load. Kobori [11] published a detailed overview of these secondary effects for an insulated CI engine.

A number of theories have been proposed to explain the limited benefits from TBCs on indicated efficiency: (i) The increased wall temperature caused by TBCs would increase the heat transfer coefficient [8], especially in the presence of near wall combustion, so called convection vive [12]. (ii) Most TBCs would absorb more radiation than an uncoated metal surface does [13]. (iii) A TBC could reduce soot deposits which are a 'natural' thermal insulator, due to the higher surface temperature [14,15]. (iv) A high surface roughness and open porosity, typical for plasma sprayed coatings, can increase heat transfer [16] and slow down combustion in CI engines [17]. Finally, (v) the thermal conductivity and heat capacity of the investigated coatings might not meet the requirements for an effective insulation [18,19]. (vi) A higher charge temperature can slow down combustion due the increase in charge viscosity. Surface roughness can slow down combustion in a number of ways: reduction of large scale charge motion and turbulence from swirl and tumble [17], increased friction between spray and wall might slow down the penetration and mixing rate.

Negative effects from high surface roughness have been reported in several publications on spark ignition [20,21] as well as compression ignition engines [22,23]. To mitigate the negative impact of surface roughness in a CI engine, Kawaguchi et al. [19] limited the application of their new TBC to the piston top surface, excluding the bowl as shown in Figure 3. However, the reported efficiency improvement of this coating was for a low engine load, while the authors used high load conditions to prove the negative effect of surface roughness in the bowl. The typical reported difference in engine efficiency is about 1-3% between a smooth and rough surface finish. However, in some cases no effect was shown, or efficiency deteriorated as much as 6%. Also for experiments with surface roughness the results varied, for similar reasons as described in the previous paragraph.

Figure 3. Piston from Toyota with a TBC of anodized aluminum [19].

The published experimental results, particularly for CI engines, do not show a clear consensus with respect to the effectiveness of thermal barrier coatings and the negative impact of surface roughness on indicated efficiency.

2.3 Research questions

Reduction of heat losses in internal combustion engines, especially diesel engines has been subject of investigation for a long time. In the early days, the target was to create an adiabatic engine with high efficiency and no need for cooling. Stainless steel and air gap insulated pistons and cylinderheads were tested, as well as ceramic thermal barrier coatings. The results from these investigations were not as positive as expected; the thermal efficiency was even reduced in some cases. Since then numerous configurations have been tested and simulated with a large range of varying outcome. No means for reduction of heat transfer with insulation has made its way to the market today, apart from one engine from Toyota on a limited market.

Research questions:

1) Why do today's thermal barrier coatings not improve indicated efficiency? (confirm the status of state of the art TBC in engine experiments)
2) What are the requirements for a thermal barrier coating to increase indicated efficiency by 2%?
3) How can recent developments in plasma sprayed coatings for aerospace be used in internal combustion engines?

2.3.1 Combustion chamber deposits

This section about combustion chamber deposits originates from a separate literature study and is not published. However, it is highly relevant in the context of thermal insulation because 1) soot deposits effectively insulate the combustion chamber and improve indicated efficiency and 2) soot deposit formation depends on the surface temperature and interacts with the presence of thermal barrier coatings and 3) soot deposits might show a way forward to create more effective TBCs.

Combustion chamber deposits (CCD) are a normal occurrence in internal combustion engines. These deposits originate from incomplete combustion products like soot and hydrocarbons. In compression ignition engines, the main source for deposits is soot from fuel burned under local rich conditions. In spark ignition engines, where the fuel burns stoichiometric, lubrication oil and fuel wall condensates are the main sources of deposits. The importance of deposits for heat transfer is that they can possess a low thermal conductivity. Already in early experiments by Hohenberg [24] and Woschni [14], measuring and quantifying heat losses from the combustion chamber, the insulating properties of soot deposits were recognized.

Soot deposits might cover surface roughness, or they might follow or even enhance the underlying roughness (indication from my own pictures, where the burning jet hits the wall). The process that enhances the surface roughness could be similar to the process for suspension plasma spraying, building feather like structures, depositing particles on the sides of the 'bumps'.

The smallest elements in soot are spherules with an internal structure of carbon platelets, similar to graphite. The typical size of these spherules is 10-50 nm. Soot particles consist of agglomerated spherules and have a typical size range of 10-200 nm. Unburned hydrocarbons condensate on the particulates, resulting in a range of dry to sticky/wet soot particles, depending on the amount and kind of hydrocarbons

absorbed. The final soot particles themselves have low porosity and the density is close to that of graphite. However, when the soot is deposited on the combustion chamber surface, the porosity of the deposit can adopt quite high values [25].

In Table 2, typical physical properties of soot are listed, as well as the properties of carbon, graphite and diamond. The heat capacity is very similar for the different forms of carbon, increasing somewhat for the more complex molecules as expected. But the conductivity of carbon and soot is much lower then that of graphite and diamond, which are actually very good heat conductors. As soot is formed into a deposit, the heat conductivity can become even lower, which is related to the level of porosity. As a result, the range of thermal conductivity of soot varies from modern thermal barrier coatings, around 1.5 W/m.K, down to very low values of 0.07 W/m.K. Although soot is a thermal insulator, it absorbs radiation very well. It is not known how this affects total heat transfer. The soot layer might get very hot from the radiation, but not effectively transmit the heat to the metal surface below due to the low thermal conductivity.

Table 2. Physical properties for soot deposits, in comparison with carbon, graphite and diamond. Sources: [26–29].

	c_p [J/kg.K]	k [W/m.K]	Porosity [%]	ρ [Jkg/m^3]
Soot deposits	840-1260	0.07-1.6	5-95	170-2180
Carbon	600-1000	1.7	-	1800-2100
Graphite	708-717	119-168	-	1900-2300
Diamond	427-516	900-3320	-	3500

The mechanisms for deposition have been studied by a number of researchers in experiments and simulations [27,29,30] The main process for deposition is found to be thermophoresis. The relatively large soot particles experience a force from the surrounding gas molecules due to the temperature gradient in the near-wall charge. The hotter and faster moving gas molecules further away from the wall transfer a higher impulse to the particles compared to the colder and slower gas molecules near the wall. The net force pushes the soot particles towards the wall surface. The other important process involved in deposit formation is oxidation. Combustion chamber deposits are oxidized when high temperature and excess oxygen are available. The resulting deposit layer growth is thus a balance between the deposition by thermophoresis and deposit removal by oxidation. A cold wall will give a thicker deposit layer compared to a hot wall: the soot deposition rate from thermophoresis is high, the oxidation rate is low. Experimental results with thermal barriers confirm this effect: a hot TBC wall showed less soot deposits [14]. The deposit layer thickness is also changing with engine operating conditions. For example, high sooting conditions will create more deposits, high engine loads and combustion temperature will enhance soot oxidation.

As deposit formation is governed by local near wall conditions, the deposit thickness and properties will differ depending on the location in the combustion chamber.

Typically, most deposits are formed in the piston top land and on the surfaces that come in contact with burning sprays. Outside of these regions, the deposits are relatively thin. The typical deposit layer thickness is between 30 and 150 µm [28,29,31,32], where a thinner layer in general has higher porosity and the thicker layer is more solid. Deposit formation times also greatly vary. It appears that the thicker, more solid deposits can take many hours to stabilize, while the thin porous soot layers can be stable in a timescale of minutes [24,27,28].

Pure soot is likely to give a deposit with a loose, porous structure, while soot with a high amount of unburned hydrocarbons is likely to stick together, for example where the fuel spray interacts with the piston bowl as shown in Figure 4. Even chemical reactions can occur between hydrocarbons and especially oil additives that bind the unburned products to a solid layer. The latter is typically seen in the piston top land area were lubrication oil is present.

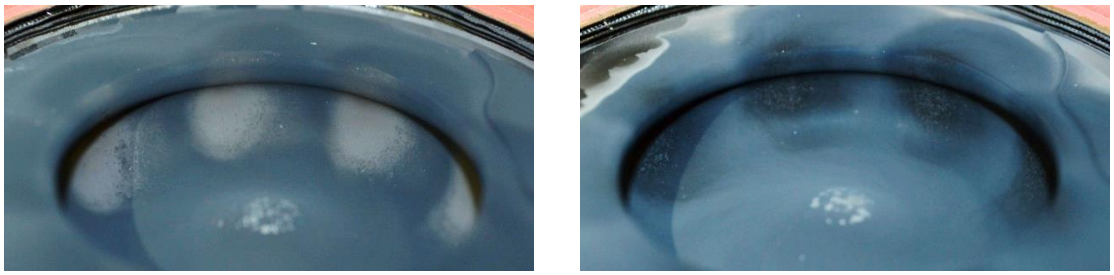

Figure 4. Soot deposits in the piston bowl. The left piston has been run at 5 bar IMEP, 1500 rpm with high EGR, the right piston at 20 bar IMEP, 3000 rpm without EGR.

When doing engine experiments involving heat transfer, the effect of deposits cannot be ignored. If possible, the amount of deposits should be controlled when comparing different engine hardware. This can be done by setting fixed initial conditions (ex. cleaned surfaces) and applying well controlled engine operating conditions with a well defined running duration in each operating point. However, different hardware might affect the composition and layer thickness of the deposits. Being aware of and accounting for deposit effects is a necessary part of the experimental work on heat transfer in combustion engines.

3 Method

The purpose of the experimental method was to assess, with high accuracy, the effect of thermal barrier coatings on fuel consumption and heat losses. The experiments should confirm the effectiveness of state of the art TBCs, applied in a modern light duty diesel engine.

The chosen method was to test the thermal barrier coatings in a single cylinder engine. The analysis was mainly based on cylinder pressure measurements. From these measurements the indicated work and apparent rate of heat release were calculated. With the measurement of the fuel consumption and exhaust emissions an energy balance for the high pressure cycle could be made. This energy balance shows the indicated efficiency, wall heat losses, exhaust enthalpy losses and emission losses. As a complement to the calculated heat losses, the heat losses to the piston cooling oil were measured as well.

The compression ratio is an important parameter for the cylinder pressure analysis. To calculate the compression ratio the clearance volume must be known. Normally this volume is determined by measurement of the the piston and cylinderhead volumes. In case of the coated pistons, this method did not give accurate results due to the porosity of the thermal barrier coatings. Therefore an alternative method to determine the compression ratio was developed.

The measured data was modeled using multiple linear regression to increase the precision of the indicated efficiency estimation. The model could also be used to isolate different factors that influence the efficiency, heat losses and emissions.

In the method section a short summary is presented for each topic. The two papers attached to this thesis contain the details.

3.1 Cylinder pressure analysis

The basis for calculation of the indicated efficiency, heat losses and exhaust enthalpy is the measured cylinder pressure. From the cylinder pressure the apparent rate of heat release (aRoHR) or Q_n can be calculated according to equation (15). The derivation of this equation can be found in Heywood [25], page 510. The ratio of specific heats κ is a function of gas composition and temperature according to the publiction by Hohenberg and Killman [33].

$$\frac{dQ_n}{d\theta} = \frac{\kappa}{\kappa - 1}\, p\, \frac{dV}{d\theta} + \frac{1}{\kappa - 1}\, V\, \frac{dp}{d\theta} \tag{15}$$

The law for the conservation of energy gives equation (16), the energy input from the fuel is equal to the the indicated work, the wall heat losses and the exhaust enthalpy.

$$Q_f = W_{i,g} + Q_w + H_{exh} \tag{16}$$

The energy in the fuel in not completely converted to heat, some energy is lost in incompletely burned emissions in the exhaust (Equation (17)).

$$Q_f = m_f\, Q_{LHV} - \, m_{CO}\, Q_{LHV_{CO}} - m_{THC}\, Q_{LHV_{THC}} \tag{17}$$

The indicated work, wall heat loss and exhaust enthalpy can now be calculated with equations (18), (19) and (20).

$$W_{i,g} = \int_{-180}^{180} p \frac{dV}{d\theta} d\theta \tag{18}$$

$$Q_w = Q_f - Q_n \tag{19}$$

$$H_{exh} = Q_n - W_{i,g} \tag{20}$$

The cumulative net apparent heat release Q_n is calculated for the part of the cycle where the intake and exhaust valves are closed. It is assumed that heat losses before intake valve closing and after exhaust valve opening are very small compared to the rest of the high pressure cycle.

$$Q_n = \int_{-145}^{145} \frac{dQ_n}{d\theta} d\theta \tag{21}$$

3.2 Single cylinder research engine

The single cylinder research engine is based on a medium duty base engine from AVL and combined with the combustion system of a Volvo light duty diesel engine, with specifications according to Table 3. Details of the measurement system are listed in Table 4, and a picture of the engine is shown in Figure 5.

Table 3. Single cylinder engine specifications.

Test engine type	**AVL 5812**
Displaced volume	492 cc
Stroke	93.2 mm
Bore	82.0 mm
Compression ratio (nominal)	15.5
Bowl type	re-entrant
Number of Valves	4
Swirl Number (Honeycomb)	2.0 to 3.2
Nozzle hole number x diameter	8 x 0.125 mm
Included spray angle	155 degrees
Fuel injection system	Common Rail, 2500 bar
Injector actuator type	Solenoid

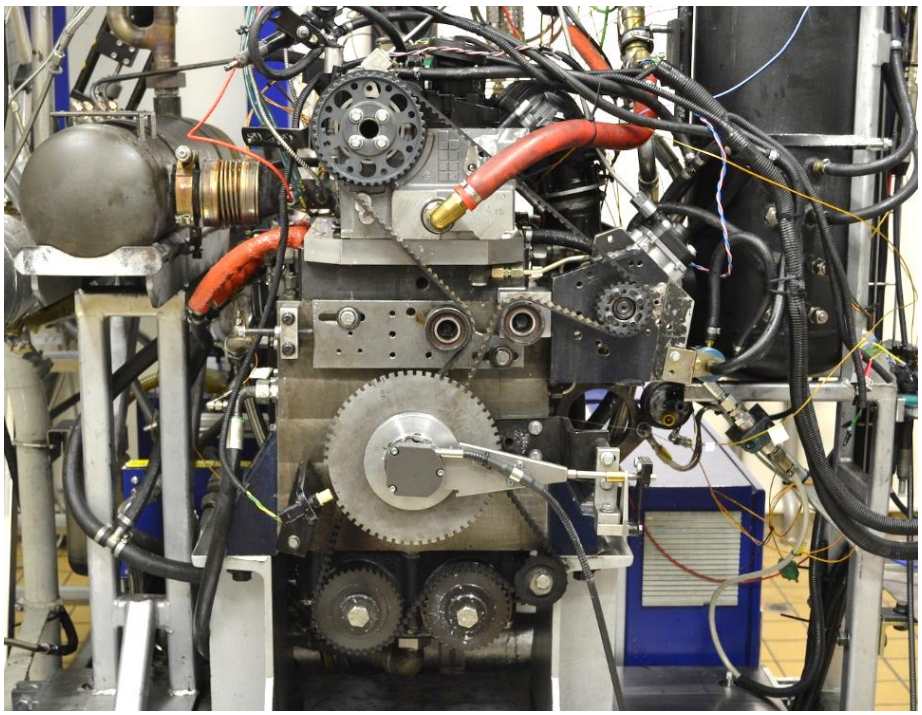

Figure 5. Single cylinder diesel research engine at Volvo Cars.

Table 4. Specification of the measurement system.

Variable	**Sensor / instrument**
Cylinder pressure	AVL GH14P
Crank angle position	AVL 365C
Intake temperature	Pentronic PT100
Intake pressure	GEMS 4000 0-6 bar abs
Exhaust pressure	GEMS 4000 0-10 bar abs
Fuel mass flow	AVL 733 fuel balance
Emissions, EGR	Horiba MEXA-7100DEGR
Intake air flow	Aerzen Zf 038.06

3.3 Compression ratio determination

An alternative method to determine the compression ratio was needed because the volume of the coated pistons could not be measured correctly with the standard measurement using a liquid. This was due to the porosity of the thermal barrier coatings which was not or only partly filled by the liquid. The compression ratio estimation uses cylinder pressure traces from a motored engine and is based on a masters thesis by Krieg [34]. The method was is described in detail in Paper I.

Figure 6 illustrates the effect of porosity of a thermal barrier coating on the compression ratio, provided that the coated piston has the same surface contour as an uncoated piston. The volume in the pores adds extra volume to the clearance volume which reduces the compression ratio.

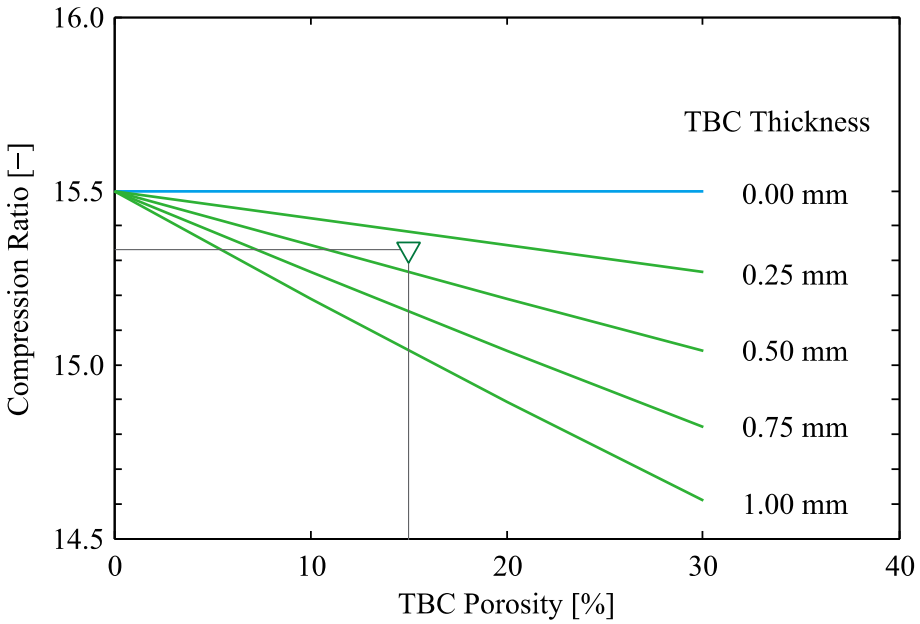

Figure 6. Compression ratio reduction as a function of TBC thickness and porosity. The green triangle indicates typical values for a plasma sprayed zirconia TBC.

Calculation of the apparent rate of heat release is sensitive for the value of the compression ratio. In Figure 7 the aRoHR is plotted for the reference piston and a coated piston. The yellow curve for the coated piston with the measured compression ratio shows an unfeasable heat loss before start of combustion. It can also be seen that the error in the compression ratio gives similar effects as the thermal barrier coating on the apparent rate of heat release.

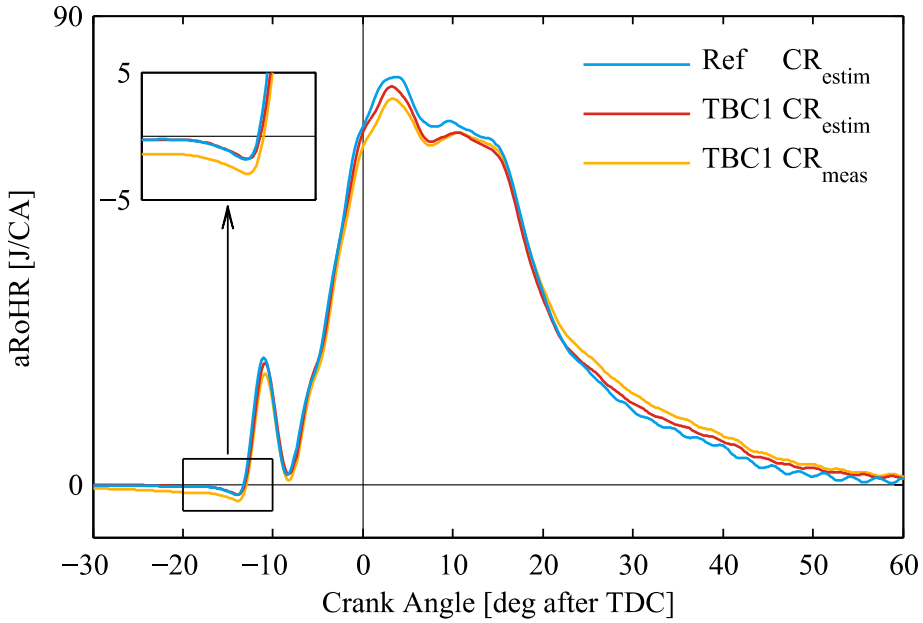

Figure 7. Apparent rate of heat release for the reference piston (Ref) and a piston coated with alumina (TBC1), calculated with measured and estimated values for the compression ratio.

3.4 Piston oil cooling heat flux measurement

To complement the calculated heat loss from the thermodynamical assessment, the heat flow to the piston cooling oil was calculated from the temperature increase of the oil in the cooling gallery and the piston cooling oil flow, according to Equation (22). The typical heat flux to the piston cooling oil is 60 to 70% of the total heat flux to the piston for a piston with a cooled ring carrier [35].

$$\dot{Q}_{oil} = \rho_{oil}\, c_{p,oil}\, \dot{V}_{oiljet}\, (T_{oilexit} - T_{oiljet}) \qquad (22)$$

The amount of heat transferred to the piston cooling oil is a measure of the thermal resistance between the piston surface and the cooling oil in the gallery. Adding a TBC or modification of the piston surface roughness for example, will change the thermal resistance, which can be measured by a change of the heat loss to the piston cooling oil. There will be differences in the thermal resistance between uncoated pistons as well, due to tolerances in geometry and contact resistance between the stainless steel cooling gallery and the aluminum of the piston. However, these differences are expected to be small in comparison to the effect of the TBCs. If there is a significant influence, this will be seen in the accuracy of the modeled data.

The oil jet in this setup is likely to be laminar (Re = 2900) with very little dispersion within the short distance to the inlet of the cooling gallery. Most of the oil from the nozzle is expected to enter the cooling oil gallery. The main influence on the capturing efficiency would be increased backflow with higher engine speed [36].

To improve the accuracy of the exit oil temperature measurement, a short pipe was added to the cooling oil gallery exit, directing the oil flow to the temperature sensor,

shown in Figure 8. The sensor itself was mounted in a funnel that collected the oil, thereby minimizing the cooling effect from the surrounding crankcase gas. The principle for the measurement was adopted from Dahlström et al. [37].

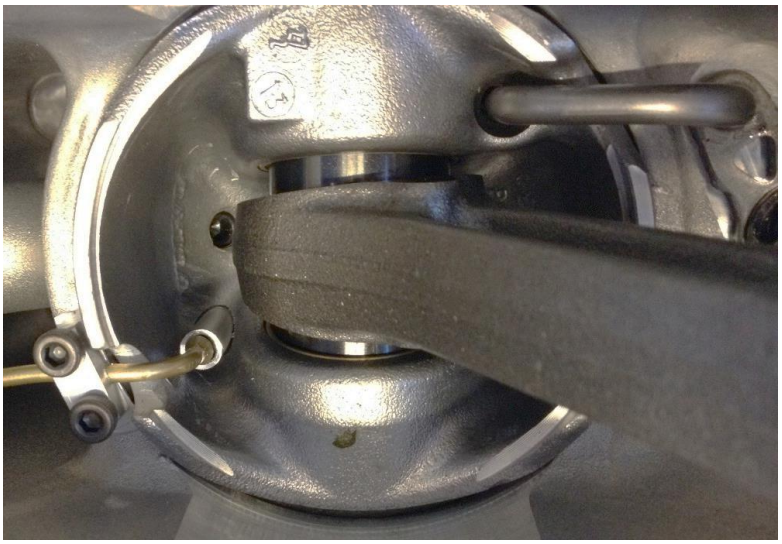

Figure 8. Bottom view of piston and cylinder with the oil cooling jet pipe on the top right and the temperature sensor mount on the left bottom [37].

3.5 Engine operating points and test sequence

Three engine operation points (EOP) were chosen to represent low, medium and high load conditions. Table 5 lists the engine speed, fuel mass, fuel pressure and injection pressure as well as intake and exhaust pressure. All load points were run with one pilot fuel injection of 2 mg.

Table 5. Engine operating points for the experiments.

Operating point	Speed [rpm]	Fuel [mg/str]	Pintake [bar]	Pexhaust [bar]	Pfuel [bar]	CO_2_in [%]	IMEP [bar]
C	3000	2 + 58	2.6	2.8	1500, 2000	0	20
B	1500	2 + 28	1.7	1.9	1000	0, 1.5, 3	10
A	1500	2 + 13	1.3	1.5	500	0, 1.5, 3, 4	5

In each of the three engine load points a few parameter variations were included. The parameters were swirl level, fuel injection pressure and EGR level because these parameters have an effect on heat losses. A second purpose of using EGR was to create an increasing amount of soot deposits on the combustion chamber walls during

a test run. These soot deposits have an insulating effect and this will be compared with the insulating effect of the thermal barrier coatings.

Each hardware setup was measured in 26 consecutive engine operation points. The test run started with motoring conditions for EOP A, B and C. Thereafter the high load point C was run with a variation of fuel pressure, followed by motoring. The medium load point B was run with a variation of EGR and swirl, again followed by motoring. Finally the low load point was run, also with a variation of EGR and swirl. The test sequence concluded with motoring. The purpose of the motored operating points was to calculate the compression ratio and to evaluate the motored heat losses with TBCs and different soot deposit levels. The test run was automated with fixed times for the stabilizing of boundary conditions and the recording of measurements. A detailed description of the complete test run setup can be found in both papers I and II.

3.6 Statistical data modeling with MLR

Multiple linear regression (MLR) is a statistical method that fits a linear equation to a result (response) from multiple inputs (factors). The input factors can be continuous or categorical with multiple levels. The factors are scaled by their range and centered by their median, to be able to compare the relative contribution of each factor. It is possible to combine factors to capture interactions, but this was not needed in this investigation.

A number of benefits come from modeling of the measured data:

- Combining data from multiple measurements in each engine operating point makes the estimation of the results more precise.
- Fitting the a model to the data creates correlation coefficients for the different input factors. With these coefficients, the contribution of each input factor can be studied separately.
- With the model it is possible to make predictions and study new combinations of the input factors.
- The model provides 95% confidence intervals for the calculated results and for the model coefficients.

In study described in Paper II, MLR models were created for the measurement results from the fired and motored energy balance, the combustion delay and the exhaust emissions. The input factors for the models were piston surface coating, surface roughness, compression ratio and factors that represent the experimental conditions. The software used for the statistical analysis was MODDE 11 from Umetrics.

4 Tested thermal barrier coatings

The choice of the investigated thermal barrier coatings was based on a short literature study and an investigation of possible suppliers. The purpose was to find state of the art coatings that represent typical thermal barrier coatings for automotive application. The selected TBCs were plasma sprayed zirconia, anodized alumina and two types of coatings from an aftermarket coating company with the name Swaintech.

4.1 Zirconia and alumina

Plasma sprayed zirconia is by far the most researched thermal barrier coating. It originates from the gas turbine industry and has very good mechanical properties and also quite good thermal properties. Anodized aluminum has gained renewed interest as a thermal barrier coating due to the work presented by Kawaguchi et al. [19], from Toyota.

Supplier for the zirconia coating was University West in Trollhättan. This University has a tight cooperation with the gas turbine industry and is specialized in plasma spraying processes. The alumina coating was supplied by Mahle, who was the piston supplier for the Volvo diesel engine. These two coatings and their application on the pistons are described in detail in Paper II.

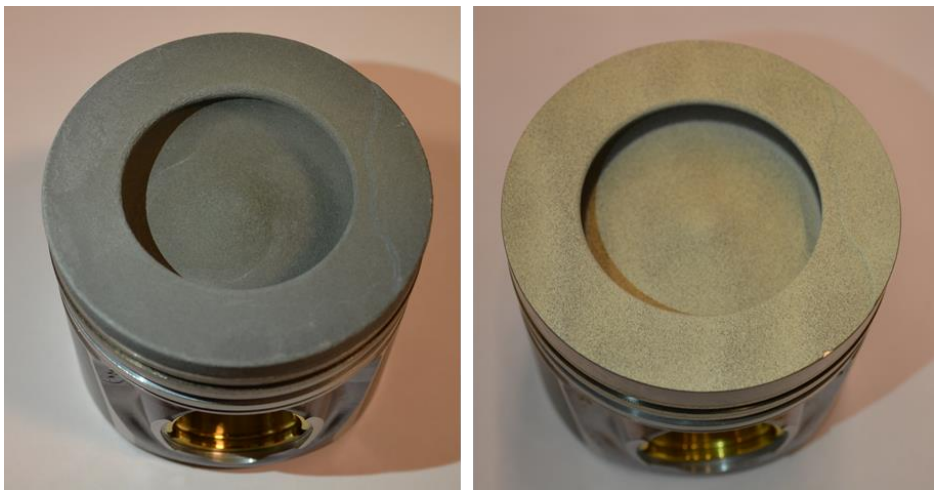

Figure 9. Pistons with Thermal Barrier Coatings.
Left: hard anodized aluminium oxide. Right: plasma sprayed zirconium oxide.

The structure of the two thermal barrier coatings is very different as can be seen in pictures of the cross section made with an electron microscope, in Figure 10 and Figure 11.

The plasma sprayed zirconia is applied on a bond coating to ensure adhesion and compatibility with respect to thermal expansion. The zirconia is stacked in the form of pancakes or 'splats'. Cracks or spaces parallel to the aluminum surface reduce thermal conduction, but can also initiate mechanical failure of the coating. The target thickness of the zirconia layer was 200 µm. The picture also shows the relatively rough surface structure.

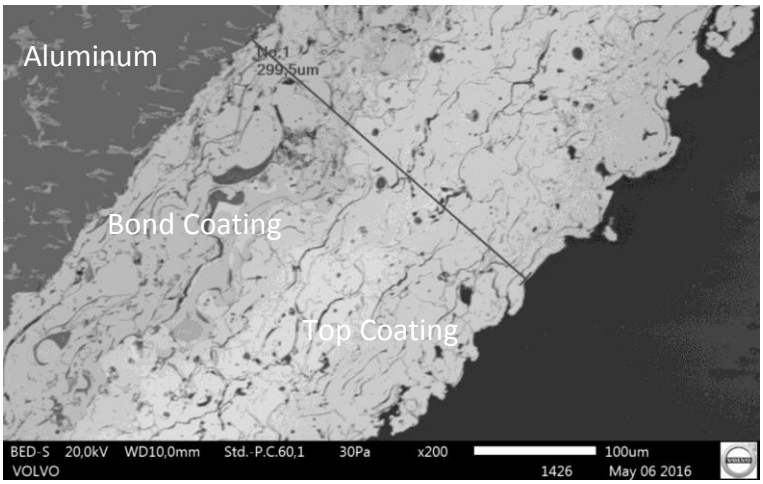

Figure 10. Electron microscope image of cross section of plasma sprayed zirconia.

The alumina layer in Figure 11 is grown from the aluminum substrate with an electrochemical process. The volume of the aluminum oxide is twice that of the aluminum after reacting with oxygen. To reach the target thickness of 200 µm, 0.1 mm of the substrate was consumed. The coating had low mechanical strength, especially at the surface. The structure of the layer depends to a high degree on the settings and chemicals used in the anodizing process. Surface roughness measurements showed a similar (high) surface roughness for both the zirconia and alumina coatings.

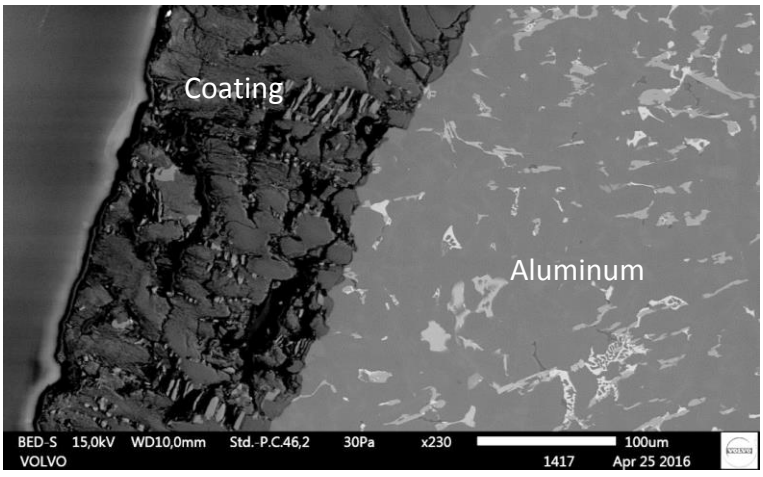

Figure 11. Electron microscope image of a cross section of anodized alumi

4.2 Aftermarket thermal barrier coatings

Two types of coating were ordered from a company with the name Swaintech based in the US. The names of the coatings were 'Gold' and 'TBC', see Figure 12. Application of these coatings is by spraying a solution on the substrate which is dried and hardened in an oven at moderate temperature. The typical thickness of these coatings was 30 to 60 µm.

On the website of Swaintech improved durability and power is claimed for SI racing engines and increased power and fuel economy is promised for truck engines. These coatings were also tested in the single cylinder engine. The experimental data did not show any significant effect on the engine efficiency, heat losses and emissions. The results of this investigation were interesting, but not published.

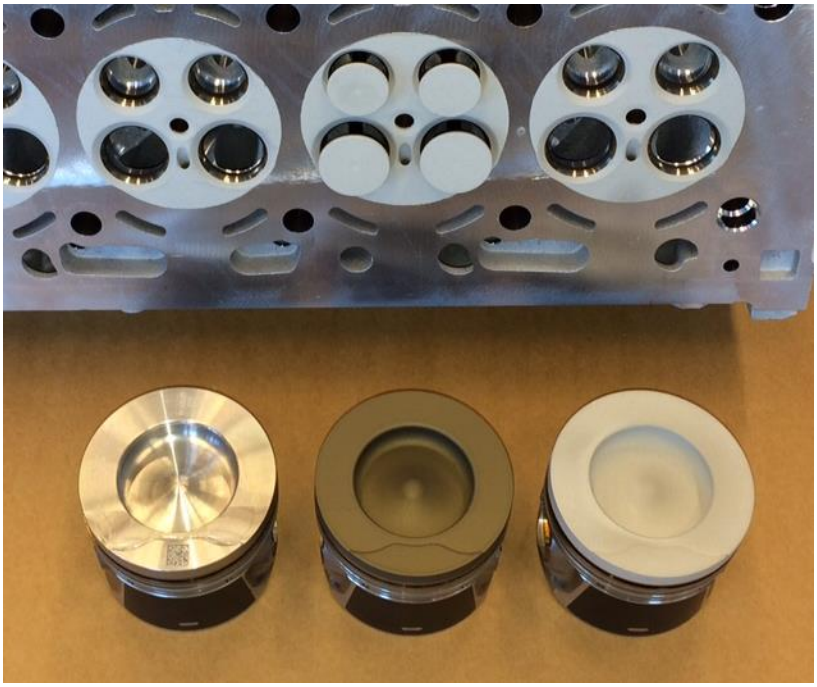

Figure 12. Thermal barrier coated cylinderhead, valves and pistons by Swaintech. The piston on the left is an original uncoated piston.

5 Contributions to the field

5.1 Paper I

"A Method to Evaluate the Compression Ratio in IC Engines with Porous Thermal Barrier Coatings"

The compression ratio is an important engine design parameter. It determines to a large extend engine properties like the achievable efficiency, the heat losses from the combustion chamber and the exhaust losses. The same properties are affected by insulation of the combustion chamber. It is therefore especially important to know the compression ratio when doing experiments with thermal barrier coatings (TBC). Another important reason to know the correct compression ratio is its use in the calculation of the apparent rate of heat release. An error in the value for the compression ratio results in deviations of the calculated heat release that are similar to the effects of TBCs.

In case of porous TBCs, the standard methods to measure the compression ratio can give wrong results. When measuring the compression ratio by volume, using a liquid, it is uncertain if the liquid fills the total porous volume of the coating. And for a thermodynamic compression ratio estimation, a model for the heat losses is needed, which is not available when doing experiments with insulation.

The subject of this paper is the evaluation and further development of an alternative method to assess the compression ratio. This method was described in a thesis work by Tomas Krieg in 1990 [34]. It is based on motored cylinder pressure data like other thermodynamic methods but does not need a model for the heat losses.

Two important modifications were made to make the estimation work properly. The first one was the addition of elastic engine deformation caused by cylinder pressure and inertial forces. The elasticity constant was determined from CAE models and measurements in an optical engine.

The second modification was related to the determination of the crank angle position for the maximum of the motored heat losses. This parameter is central in the method. The assumption in the original paper that the heat loss maximum always occurs between the crank angle position for maximum charge temperature and maximum charge pressure does not hold. The reason for this is the decay of the charge turbulence which is engine specific and has a big influence on the motored heat losses. The turbulence development of the cylinder charge is depending on engine design and motoring conditions and cannot be modeled in a simple way. The solution was to measure the crank angle position for the maximum heat losses for an uncoated reference piston with a known compression ratio and assume that it would be the same for the coated pistons. This assumption was verified for differences in surface roughness and heat losses.

The validation and application of the alternative method for compression ratio estimation was done with data from experiments involving two types of porous TBCs, performed on a light duty single cylinder diesel engine. The results are very repeatable and indicate that the proposed method accurately predicts the compression ratio for porous thermal barrier coatings.

5.2 Paper II

"Evaluation of thermal barrier coatings and surface roughness in a single cylinder light duty diesel engine"

The effect of two thermal barrier coatings (TBC) and their surface roughness on heat transfer, combustion and emissions was investigated in a single cylinder light duty diesel engine. The evaluated TBC materials were plasma sprayed yttria stabilized zirconia and hard anodized aluminum, which were applied on the piston top surface.

The background for this investigation was the large spread in reported data for the effectiveness of thermal barrier coatings and the need for an accurate assessment.

The main tool for the investigation was cylinder pressure analysis of the high pressure cycle, from which the apparent rate of heat release, indicated efficiency and heat losses were derived. For verification of the calculated wall heat transfer, the heat flow to the piston cooling oil was measured as well. Exhaust emission measurements were also performed.

Application of TBCs can influence engine operating conditions like charge temperature and ignition delay. This is one of the reasons for the large spread in data for efficiency improvements from TBCs found in literature. Therefore extra attention was paid to choosing stable and repeatable engine operating points and the test run was automated to improve repeatability. The experimental data was modeled using multiple linear regression (MLR) to further improve the accuracy. Another advantage of the modeling was that it was possible to isolate the effects of the coatings, surface roughness, compression ratio and soot deposits.

With this method it was possible to determine the indicated efficiency with a 95% confidence interval of ±0.1 percentage point. Efficiency differences as low as 0.2 percentage point could be distinguished between the different pistons.

Both tested thermal barrier coatings showed a reduction of cycle averaged wall heat losses and an increase in exhaust enthalpy, and a decrease in indicated efficiency.

Analysis revealed that the high surface roughness of the tested TBCs led to increased wall heat losses and a delayed combustion. An increase of surface roughness R_a from 0.2 µm to 7.4 µm resulted in a fuel consumption increase of up to 1%.

The effect of soot deposits on motored heat losses was also derived from the MLR model. The thermal insulation of the soot deposits was significantly better than the thermal insulation of the tested TBCs. This effect was known in literature, but has not been quantified in this way before.

Finally some results for the emissions: the surface roughness and TBCs had a significant impact on the hydrocarbon emissions, especially for low load engine operation, while their effect on the other exhaust emissions was relatively small.

6 Future work

From the previous literature study and experiments it became clear that further development is needed on thermal barrier coatings to achieve significant benefits in engine efficiency. The surface of a TBC should have a low surface roughness and it should be sealed to avoid penetration of the hot gas. Thermal conductivity and volumetric heat capacity of TBCs should be reduced from typical values of 1.5 W/m.K and 2.7 MJ/m^3.K to values below 1.0 W/m.K and 1.0 MJ/m^3.K respectively.

Therefore the next steps in the research are to investigate the effect of sealing and polishing porous plasma sprayed coatings. This will be combined with new materials and new material structures developed for aerospace applications with improved properties for thermal insulation.

Sealing of the surface will be done in three different ways: 1) by application of a polysilazane which cures to a ceramic at elevated temperatures, 2) by applying a dense ceramic top layer or by 3) applying a dense metal top layer. An advantage of the dense metal top layer might be that it could reflect more radiated heat than a ceramic top layer.

Gadolinium is a new material used in TBCs for aerospace applications. It has lower thermal conductivity and lower heat capacity compared to zirconia and will be subject of investigation for engine application. New structures of the ceramic coatings can be made with the suspension plasma spraying process (SPS). This process has been developed for increased durability; the resulting material structure it is more compliant to thermal expansion of the substrate. A second advantage is the low thermal conductivity compared to the current air plasma spraying (APS).

The work on the coatings will be done in cooperation with University West in Trollhättan. Their Production Technology Centre has a long experience of developing plasma-sprayed thermal barrier coatings for the Aerospace industry. The new thermal barrier coatings will be evaluated with single cylinder engine experiments using the method that was developed and used for the previous experimental campaign, described in this thesis.

References

1. Cengel, Y.A. and Ghajar, A.J., “Heat and Mass Transfer, Fundamentals & Applications,” McGraw-Hill, ISBN 978-0-07-339812-9, 2011.
2. Woschni, G., “A Universally Applicable Equation for the Instantaneous Heat Transfer Coefficient in the Internal Combustion Engine,” SAE Technical Paper, 1967, doi:10.4271/670931.
3. Kamo, R. and Bryzik, W., “Adiabatic Turbocompound Engine Performance Prediction,” SAE Technical Paper 780068, 1978.
4. Bryzik, W. and Kamo, R., “TACOM/Cummins Adiabatic Engine Program,” SAE Technical Papers, 1983.
5. Kamo, R., Bryzik, W., and Glance, P., “Adiabatic Engine Trends-Worldwide,” SAE Technical Papers, 1987, doi:10.4271/870018.
6. Kamo, R., Assanis, D., and Bryzik, W., “Thin Thermal Barrier Coatings for Engines,” SAE Technical Paper, 1989.
7. Morel, T., Keribar, R., and Blumberg, P.N., “Cyclical Thermal Phenomena in Engine Combustion Chamber Surfaces,” SAE Technical Paper 850360, 1985, doi:10.4271/850360.
8. Woschni, G., Spindler, W., and Kolesa, K., “Heat Insulation of Combustion Chamber Walls - A Measure to Decrease the Fuel Consumption of IC Engines?,” SAE Technical Paper, 1987, doi:10.4271/870339.
9. Amann, C.A., “Promises and Challenges of the Low-Heat-Rejection Diesel,” J. Eng. Gas Turbines Power 110(July):475–481, 1988.
10. Jaichandar, S. and Tamilporai, P., “Low Heat Rejection Engines – An Overview,” SAE Technical Paper, 2003, doi:10.4271/2003-01-0405.
11. Kobori, S., Kamimoto, T., and Luta, M.T., “Combustion in Low-Heat-Rejection Diesel Engines,” JSME Int. J. 35(1), 1992.
12. Lang, T. and Germerdonk, R., “Einfluss von wandnahen exothermen Reaktionen auf den konvektiven Wärme- fluss (Convection vive),” Chemie Ing. Tech. 61(11):918–919, 1989.
13. Mendera, K.Z., “Effectiveness of Plasma Sprayed Coatings for Engine Combustion Chamber,” SAE Technical Papers, 2000, doi:10.4271/2000-01-2982.
14. Woschni, G. and Huber, K., “Influence of soot deposits on combustion chamber walls on heat losses in diesel engines,” SAE Technical Paper 910297, 1991, doi:10.4271/910297.
15. Cheng, S.S., “A Physical Mechanism for Deposit Formation in a Combustion Chamber,” SAE Technical Paper, 1994, doi:10.4271/941892.
16. Mruk, A., Jordan, W., Taler, J., Lopata, S., et al., “Heat Transfer Through Ceramic Barrier Coatings Used in Internal Combustion Engines,” SAE Technical Papers, 1994, doi:10.4271/941779.

17. Tree, D.R., Oren, D.C., Yonushonis, T.M., and Wiczynski, P.D., "Experimental Measurements on the Effect of Insulated Pistons on Engine Performance and Heat Transfer," SAE Technical Papers (412), 1996, doi:10.4271/960317.

18. Wallace, F.J., Kao, T.K., Tarabad, M., Alexander, W.D., et al., "Thermally Insulated Diesel Engines," Proc. Inst. Mech. Eng. Part A, J. Power Energy 97–105, 1984.

19. Kawaguchi, A., Iguma, H., Yamashita, H., Takada, N., et al., "Thermo-Swing Wall Insulation Technology; - A Novel Heat Loss Reduction Approach on Engine Combustion Chamber," SAE Technical Paper 2016-01-2333, 2016, doi:10.4271/2016-01-2333.

20. Tsutsumi, Y., Nomura, K., and Nakamura, N., "Effect of Mirror-Finished Combustion Chamber on Heat Loss," SAE Int. 902141, 1990.

21. Memme, S. and Wallace, J.S., "The influence of thermal barrier coating surface roughness on spark-ignition engine performance and emissions," *Proceedings of the ASME 2012 Internal Combustion Engine Division Fall Technical Conference*, ASME, Vancouver: 893–905, 2012, doi:10.1115/ICEF2012-92078.

22. Tree, D.R., Wiczynski, P.D., and Yonushonis, T.M., "Experimental Results on the Effect of Piston Surface Roughness and Porosity on Diesel Engine Combustion," SAE Technical Paper, 1996, doi:10.4271/960036.

23. Osada, H., Watanabe, H., Onozawa, Y., Enya, K., et al., "Experimental Analysis of Heat-Loss with Different Piston Wall Surface Conditions in a Heavy-Duty Diesel Engine," Comodia 9th Int. Conf., 2017.

24. Hohenberg, G.F., "Advanced Approaches for Heat Transfer Calculations," SAE Technical Paper, 1979, doi:10.4271/790825.

25. Heywood, J.B., "Internal Combustion Engine Fundamentals," McGraw-Hill, ISBN 0-07-100499-8, 1988.

26. Dietsche, K.-H. and Klingebiel, M., eds., "Bosch Automotive Handbook," 7th Editio, Robert Bosch GmbH, ISBN 978-0-470-51936-3, 2007.

27. Wolff, A., Boulouchos, K., and Mueller, R., "A computational investigation of unsteady heat flux through an I.C. engine wall including soot layer dynamics," SAE Technical Papers, 1997, doi:10.4271/970063.

28. Nishiwaki, K. and Hafnan, M., "The Determination of Thermal Properties of Engine Combustion Chamber Deposits," SAE Technical Paper Series, 2000, doi:10.4271/2000-01-1215.

29. Wiedenhoefer, J.F. and Reitz, R.D., "Multidimensional Modeling of the Effects of Radiation and Soot Deposition in Heavy-duty Diesel Engines," SAE Technical Paper, 2003, doi:ISSN 0148-7191.

30. Suhre, B.R. and Foster, D.E., "In-Cylinder Soot Deposition Rates Due to Thermophoresis in a Direct Injection Diesel Engine," SAE Technical Paper Series, 1992, doi:10.4271/921629.

31. Hopwood, A.B., Chynoweth, S., and Kalghatgi, G.T., "A Technique to

Measure Thermal Diffusivity and Thickness of Combustion Chamber Deposits In-Situ," SAE Technical Paper Series, 1998, doi:10.4271/982590.

32. Kavtaradze, R., Zelentsov, A., Gladyshev, S.P., Kavtaradze, Z., et al., "Heat Insulating Effect of Soot Deposit on Local Transient Heat Transfer in Diesel Engine Combustion Chamber," SAE Paper 2012-01-12, 2012, doi:10.4271/2012-01-1217.

33. Hohenberg, G. and Killmann, I., "Basic findings obtained from measurement of the combustion process," SAE Technical Paper 82126, 1982, doi:10.1081/E-EEE2-120046011.

34. Krieg, K., "Thermodynamische Bestimmung des Verdichtungsverhältnisses mittels eines Indizierverfahrens," Fachhochschule Aalen, 1990.

35. Kajiwara, H., Fujioka, Y., and Negishi, H., "Prediction of Temperatures on Pistons with Cooling Gallery in Diesel Engines using CFD Tool," SAE Technical Paper Series, 2003, doi:10.4271/2003-01-0986.

36. Pan, J., Nigro, R., and Matsuo, E., "3-D Modeling of Heat Transfer in Diesel Engine Piston Cooling Galleries," SAE Technical Paper Series, 2005, doi:10.4271/2005-01-1644.

37. Dahlström, J., Andersson, Ö., Tunér, M., and Persson, H., "EFFECTS OF SPRAY-SWIRL INTERACTIONS ON HEAT LOSSES IN A LIGHT DUTY DIESEL ENGINE," ASME 2015, 2015.

Symbols and acronyms

a	diffusivity
α	absorbtivity
A	surface area
B	cylinder bore
c_v	volumetric specific heat
c_p	mass specific heat
δ_p	penetration depth
e	effucivity
ε	emissivity
ϵ	surface roughness height
h_c	heat transfer coefficient
H	enthalpy
k	thermal conductivity
κ	ratio of specific heats
L	characteristic length
μ	dynamic viscosity
Nu	Nusselt number
p	pressure
Pr	Prandtl number
$\dot{Q}$	heat flux
Q_n	net apparent heat release
ρ	density
Re	Reynolds number
σ	Boltzman constant
θ	crank angle
T	temperature
U	bulk velocity
V	volume
W	work

aRoHR	Apparent rate of heat release
CA	Crank angle
CR	Compression ratio
CO	Carbon monoxide
CO_2	Carbon dioxide
EOP	Engine operating point
IMEP	Indicated mean effective pressure
LHV	Lower heating value
MLR	Multiple linear regression
NO_x	Nitrogen oxides
TBC	Thermal barrier coating
THC	Total hydrocarbons

Appended Papers I - II